

Strong Bulk Magnetic Dipole Induced Second-Harmonic Generation from C₆₀

Bert Koopmans, Anna-Maria Janner, Harry T. Jonkman, George A. Sawatzky,
and Folkert van der Woude

Laboratory of Solid State Physics, Materials Science Centre, University of Groningen,
Nijenborgh 4, 9747 AG Groningen, The Netherlands

(Received 16 July 1993)

We describe how to separate all surface, interface, and bulk tensor components in optical second-harmonic generation experiments on isotropic thin films. Using *in situ* thickness scans and group theoretical arguments concerning the bulk tensor components, we demonstrate that the second-harmonic resonance of C₆₀ at $2\hbar\omega = 3.6$ eV is of bulk character, and, quite remarkably, of magnetic dipole induced origin.

PACS numbers: 78.66.-w, 42.65.-k, 61.46.+w

Among the interesting properties of the fullerenes are their strong nonlinear optical properties. Quite some experimental effort has been made to clarify the high second and third order optical response of C₆₀ and some related materials [1-6]. In a previous paper we reported on optical second-harmonic generation (SHG) experiments on C₆₀ thin films, showing a narrow resonance at $2\hbar\omega = 3.6$ eV [6].

In this paper we present a systematic procedure to resolve all bulk, surface, and interface tensor components for an isotropic thin film system. This separation of surface vs bulk SHG contributions is known to be a fundamental difficulty in the field of surface SHG [7]. Our method makes use of the experimental data from SHG thickness scans, and an estimation of the ratio between two bulk tensor components. Using this procedure, the situation for C₆₀ is clarified for the specific case of the resonant SHG at $2\hbar\omega = 3.6$ eV. From comparison with the linear optical spectrum of C₆₀ [8,9] we expect the resonance to be dominated by the $h_g \rightarrow h_u \rightarrow t_{1u}$ diagram as indicated in Fig. 1. The forbidden $h_u \rightarrow t_{1u}$ transition energy is of the order of 2 eV, so that the total SHG diagram is at, or close to, double resonance. We demonstrate that the SHG resonance is magnetic dipole (MD) induced, and show that this is due to the spherical character of the C₆₀ molecule. To our knowledge this is the first direct evidence for such optically MD induced contributions in nonlinear optical experiments on nonconducting materials.

For third order optical experiments on C₆₀ [1-4] all involved electronic transitions are electric dipole allowed, so that the strong delocalization of the p_π molecular orbitals can give rise to high $\chi^{(3)}$ values. The situation for the second order optical response is more complicated. Although relative high SHG efficiencies for C₆₀ have been reported [4-6], the process is symmetry forbidden within the electric dipole approximation. Therefore, other mechanisms become important, that is nonlocal bulk contributions, indicated by $\tilde{\chi}^{(Q)}$ [including both MD and electric quadrupole (EQ) processes], and electric dipole allowed or field gradient induced surface contributions,

indicated by $\tilde{\chi}_S^{(D)}$ [10].

The induced nonlocal SHG polarization density in an isotropic material can be written in vector notation as

$$\mathbf{P}^{(Q)} = \frac{1}{2} \chi_3^{(Q)} \nabla(\mathbf{E} \cdot \mathbf{E}) + \chi_4^{(Q)} (\mathbf{E} \cdot \nabla) \mathbf{E} + \chi_2^{(Q)} \mathbf{E}(\nabla \cdot \mathbf{E}), \quad (1)$$

where [10] $\chi_1^{(Q)} = \chi_{xxxx}^{(1)}$, $\chi_2^{(Q)} = \chi_{xxyy}^{(Q)}$, $\chi_3^{(Q)} = \chi_{xyxy}^{(Q)}$, and $\chi_4^{(Q)} = \chi_{xyyx}^{(Q)}$. The $\chi_3^{(Q)}$ contribution is known to be indistinguishable from a certain combination of surface contributions [7,10,11]. Our explicit calculations for the thin film geometry confirm this phenomenon. The $\chi_2^{(Q)}$ term is absent in the bulk because of the zero divergence of \mathbf{E} . The $\chi_4^{(Q)}$ term disappears if only a single plane wave is present inside the medium. In the thin film geometry, however, reflections from the lower interface cause a second plane wave even if the medium is irradiated by a single plane wave.

For the phenomenological description of the reflected SHG from the thin film a second harmonic sheet susceptibility $\tilde{\chi}_S^{(D)}$ is assigned to the outer surface, and $\tilde{\chi}_I^{(D)}$ to the buried interface. For an isotropic film there are only three nonzero independent sheet susceptibility components: $\chi_{\perp\perp\perp}^{(D)}$, $\chi_{\perp\parallel\parallel}^{(D)}$, and $\chi_{\parallel\parallel\parallel}^{(D)}$, with $\perp = z$ and $\parallel = x$ or y .

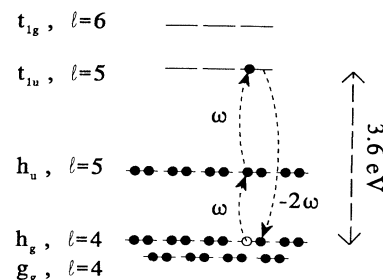


FIG. 1. Selection of the p_π molecular orbital scheme of C₆₀. The listed l values are the corresponding free-electron angular momenta. The $h_g \rightarrow t_{1u}$ excitations are responsible for the linear resonance at $\hbar\omega = 3.6$ eV for solid C₆₀. The indicated three-level diagram is the proposed dominant diagram for the SHG resonance at $2\hbar\omega = 3.6$ eV.

The bulk SHG parameters of interest are $\chi_3^{(Q)}$ and $\chi_4^{(Q)}$ of the thin film. Bulk contributions of the substrate can be included into $\tilde{\chi}_i^{(D)}$. The dielectric constant of the thin film at frequency ν ($\nu = \omega$ or 2ω) is denoted by $\epsilon(\nu)$, and the refractive index by $n(\nu)$. To tackle the problems accompanying the discontinuities of the electromagnetic fields at the interfaces, we embed $\tilde{\chi}_S^{(D)}$ and $\tilde{\chi}_I^{(D)}$ in a very thin region, with a dielectric constant equal to that of the thin film. Our results can be easily converted to the more common convention of a surface and interface dielectric constant equal to that of vacuum [12] by replacing $\chi_{\perp\perp\perp}^{(D)}$ by $\chi_{\perp\perp\perp}^{(D)}/[\epsilon(\omega)^2\epsilon(2\omega)]$, $\chi_{\perp\parallel\parallel}^{(D)}$ by $\chi_{\perp\parallel\parallel}^{(D)}/\epsilon(2\omega)$, and $\chi_{\parallel\perp\parallel}^{(D)}$ by $\chi_{\parallel\perp\parallel}^{(D)}/\epsilon(\omega)$.

Within the sketched macroscopic framework, we performed an exact calculation of the reflected SHG intensity for an incident plane wave $\mathbf{E}_{in}e^{ik \cdot \mathbf{r} - i\omega t} + \text{c.c.}$ The explicit results will be published elsewhere [13].

To resolve all distinguishable tensor components, thickness scans have to be carried out for different polarization combinations. In our experiments we employ a combination of $p \rightarrow p$ (p -polarized input, and p -polarized output), $s \rightarrow p$, $m \rightarrow s$ (mixed input polarization), and $m \rightarrow p$. The occurrence of the various resolvable combinations of tensor components for the four geometries is indicated in Table I. Note that $\chi_4^{(Q)}$ is resolvable, but $\chi_3^{(Q)}$ is not.

C₆₀ with a purity better than 99.99% was evaporated from a Knudsen cell onto fused quartz substrates, at UHV pressures below 2×10^{-9} mbar. The frequency doubled output of a Nd:YAG laser was used to pump a dye laser, producing 7 ns pulses with an energy of approximately 5 mJ/pulse and repetition rate of 10 Hz. For all experiments described in this paper $2\hbar\omega$ was tuned exactly to the 3.60 eV resonance. The linear and SHG

TABLE I. The occurrence of the resolvable tensor components for a thin film measurement in the four indicated polarization combinations. The last column shows the results (units: 10^{-13} esu) of least squares fits to the described measurement. The SH phases are relative to $\chi_4^{(Q)}$. The values between brackets have a high uncertainty of approximately 50%. The relative uncertainties of the other components are at most a few percent. The linear refractive indices can be compared to the ellipsometry results of Ren *et al.* [17]: $n(\omega) = 1.98 + 0.01i$ and $n(2\omega) = 2.17 + 0.87i$.

Component	$s \rightarrow p$	$p \rightarrow p$	$m \rightarrow s$	Experiment
		$m \rightarrow p$		
$\chi_4^{(Q)}$		●	●	1.35
$\chi_{S,\perp\perp\perp}^{(D)}$		●	●	$0.042e^{-55^\circ i}$
$\chi_{I,\perp\perp\perp}^{(D)}$		●	●	$(\sim -0.33e^{-35^\circ i})$
$\chi_3^{(Q)} + 2\chi_{S,\perp\perp\perp}^{(D)}$	●	●		$-1.34e^{-1^\circ i}$
$\chi_3^{(Q)} - 2\chi_{I,\perp\perp\perp}^{(D)}$	●	●		$-1.36e^{1^\circ i}$
$\chi_3^{(Q)} + 2\chi_{S,\perp\perp\perp}^{(D)}$		●		(~ -1)
$\chi_3^{(Q)} - 2\chi_{I,\perp\perp\perp}^{(D)}$		●		(~ -1)
$n(\omega)$	●	●	●	$2.18 + 0.01i$
$n(2\omega)$	●	●	●	$2.19 + 0.86i$

reflection, for an incident angle of 45° , was measured *in situ* during evaporation of the thin film. Absolute calibration was obtained using a reference quartz crystal. The perfect interference patterns we observed, persisting up to several μm thickness, demonstrate the high optical quality of the films, and in particular, the absence of island formation.

Figure 2 shows the data of a single thickness scan, combining the four polarization combinations. From such a scan, the parameters of Table I can be resolved. The results listed in Table I are obtained by a simultaneous fit to all geometries, for which the theoretical curves are shown in the figure. We find within a fair approximation $\chi_3^{(Q)} + 2\chi_{S,ijk}^{(D)} = \chi_3^{(Q)} - 2\chi_{I,ijk}^{(D)}$ for all i, j , and k . This can be interpreted as an indication for the marginal role of the surface and interface contributions. However, as we pointed out previously [6], this could also be due to the 180° phase difference between the surface and interface SHG susceptibilities as expected for the electric dipolar contributions of films on nonreactive substrates.

To get an idea of the relative role of surface and interface contributions, we also fitted the data with either only bulk components, or only surface and interface components. The fit using only bulk components gives good correspondence for the $s \rightarrow p$, $m \rightarrow p$, and $p \rightarrow p$ geometries, but deviates significantly for the $m \rightarrow s$ geometry as indicated in Fig. 2. On the other hand, completely neglecting any bulk contributions gives a complete mismatch for at least three of the four geometries. From this we conclude that surface and interface contributions

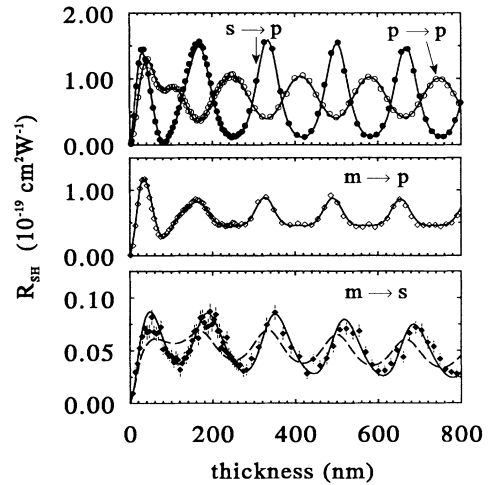


FIG. 2. The SHG reflection coefficient ($R_{SH} = I_{SH}/[I_{in}]^2$) for $2\hbar\omega = 3.60$ eV as measured *in situ* as a function of the evaporated film thickness. The four polarization combinations are measured during the same scan. The full curves are theoretical fits using the SHG parameters listed in Table I. The dashed curve indicated for the $m \rightarrow s$ geometry is a fit using only bulk contributions, demonstrating the significance of small surface and interface contributions.

are present, but the SHG is dominated by the bulk contributions. We stress that such an unambiguous identification of an isotropic bulk contribution is not possible from an ordinary single-interface reflection experiment. Finally, an important observation is that $\chi_3^{(Q)} + \chi_{\perp\parallel\parallel}^{(Q)}$ and $\chi_4^{(Q)}$ are approximately of opposite phase, and of approximate equal modulus.

In the following we use an estimated ratio of $\chi_4^{(Q)}/\chi_3^{(Q)}$ as the additional physical information necessary to obtain the full separation [10]. Note that a relation between two bulk tensor components is much more reliable (in some cases even trivial) than the relation between a bulk and a surface contribution.

Close to resonance, considering only a single degenerate three-level diagram, the bulk SH susceptibility can be written as

$$\chi_{ijkl}^{(Q)} = T_{ijkl} / [\mathcal{D}(\omega)\mathcal{D}(2\omega)], \quad (2)$$

where T_{ijkl} denotes the product of transition matrix elements summed over all degenerate diagrams, and the frequency denominators are of the form $\mathcal{D}(\nu) = \hbar\nu - \Delta E + i\hbar\Gamma$, for the proper transition energies ΔE and linewidths $\hbar\Gamma$. For the $h_g \rightarrow h_u \rightarrow t_{1u}$ diagram we have

$$T_{ijkl} = \frac{1}{2} Ne^3 \sum_{n,n',n''} \langle n | r_i | n'' \rangle \langle n'' | Q_{kl} | n' \rangle \langle n' | r_j | n \rangle, \quad (3)$$

where n , n' , and n'' are summed over the h_g , h_u , and t_{1u} states, respectively, \mathbf{r} is the displacement operator, $-e$ is the electron charge, and N is the density of molecules. The operator Q is defined as $Q_{kl} = r_k r_l$ for a pure EQ process, and $Q_{kl} = (\hat{\mathbf{f}}_k \times \hat{\mathbf{f}}_l) \cdot \mathbf{L} / im_e \omega$ for a pure MD process, where \mathbf{L} is the angular momentum operator, and m_e is the electron rest mass [14].

As a consequence of Eq. (3), a dominant EQ contribution implies $\chi_3^{(Q)} = \chi_4^{(Q)}$, since $xy = yx$. On the other hand, a dominant MD contribution leads to $\chi_3^{(Q)} = -\chi_4^{(Q)}$, because of $\hat{\mathbf{x}} \times \hat{\mathbf{y}} = -\hat{\mathbf{y}} \times \hat{\mathbf{x}}$. Therefore, the experimentally obtained ratio of $\chi_4^{(Q)} / (\chi_3^{(Q)} + \chi_{S,\perp\parallel\parallel}^{(D)}) = -1.01$, strongly suggests the dominance of a MD induced process, unless we would have a significant $\chi_{S,\perp\parallel\parallel}^{(D)}$ component.

The p_π molecular orbitals of C_{60} are closely related to free electronic wave functions for a spherical shell with a radius equal to the C_{60} radius $R = 3.5 \text{ \AA}$. Although we have very strict m -selection rules for EQ transitions ($\Delta m = \pm 2$) and MD transitions ($\Delta m = 0$), the corresponding l -selection rules are somewhat weaker, $\Delta l = 0$ or ± 2 for EQ, and $\Delta l = 0$ for MD transitions. Although $\Delta l = 0$ transitions are allowed for both EQ and MD transitions, one can show for a spherical shell that these transitions strongly support MD transitions [13]. Since the h_u and t_{1u} orbitals are both similar to the $l = 5$ spherical harmonics, we expect the indicated three-level diagram to be very favorable for MD induced processes. This agrees with our experimental observations.

A more formal way to describe the SHG processes is by considering the symmetry of the e - h pairs. Group

theory shows for the icosahedral point group that the only allowed transitions from the 1A_g ground state via EQ or MD processes, are EQ transitions to a 1H_g excitation, and MD transitions to a ${}^1T_{1g}$ excitation. The highest occupied molecular orbital—lowest unoccupied molecular orbital singlet excitations split up in a multiplet of four levels with ${}^1T_{1g}$, ${}^1T_{2g}$, 1G_g , and 1H_g symmetry, respectively. Although the identification of the (false-origin) excitations in optical absorption spectra is far from trivial, the general consensus is that the ${}^1T_{1g}$ 0-0 excitation is located close to 1.8 eV, and the 1H_g at least above 2.0 eV. This gives a second confirmation that MD processes are of importance for fundamental frequencies around 1.8 eV.

Here we want to use the opportunity to point out that our phase resolved SHG measurements [6] give strong evidence for the contribution of a doubly resonant diagram [15]. With this interpretation the resonance at the fundamental frequency agrees well with the lowest ${}^1T_{1g}$ excitation of C_{60} . Since the linewidth of the observed SH resonance, which we attribute to the MD interaction ($\hbar\Gamma_{MD} \sim 0.05 \text{ eV}$ from our phase resolved measurements), is smaller than the ${}^1T_{1g}$ - 1H_g splitting of several tenths of an eV, the SHG at resonance will be of pure MD character. This leads to a ratio $\chi_4^{(Q)}/\chi_3^{(Q)} = -1$. Straight substitution of this ratio into the results of Table I leads to $\chi_3^{(Q)} = -1.35 \times 10^{-13} \text{ esu}$, and an upper bound for $|\chi_{S,\perp\parallel\parallel}^{(D)}|$ and $|\chi_{I,\perp\parallel\parallel}^{(D)}|$ of $0.03 \times 10^{-13} \text{ esu}$ [16]. Just as for the $\chi_{\perp\parallel\parallel}^{(D)}$ components, this is at most a few percent of the bulk tensor components. We conclude that from this full separation we have indisputably shown the minor role of the surface and interface contributions.

We already gave a hand-waving argument for the relative importance of the observed MD resonance, and the probably nearby EQ resonance, based on the free-electron approximation. To check this, we explicitly carried out a calculation of T_{ijkl} for the $h_g \rightarrow h_u \rightarrow t_{1u}$ diagram of Fig. 1 on a linear combination of atomic orbitals (LCAO) base. The results are collected in Table II. In the LCAO calculation only the p_π atomic orbitals were taken into account, and we used an equal single- and double-bond hybridization of $t = 2.4 \text{ eV}$. The solid character of the C_{60} only enters through the molecular density N . For the moment we neglect any local field effects due to the dielectric environment, as well as the screening of the single electron excitations. From Table II we conclude that

TABLE II. The various T_{ijkl} 's (units: Ne^3R^4) of C_{60} for the three-level diagram $h_g \rightarrow h_u \rightarrow t_{1u}$, calculated with a LCAO approach. The MD values are specified for $\hbar\omega = 1.80 \text{ eV}$.

$ijkl$	MD	EQ
$xxxx$	0.0000	0.0258
$xyyy$	0.0000	-0.0129
$xyxy$	-0.1858	0.0193
$xyyx$	0.1858	0.0193

indeed the EQ-induced susceptibility is only 10% of the MD-induced susceptibility, so that the resonant intensities will even differ by 2 orders of magnitude.

For an absolute comparison between the experiments and the LCAO calculation we need a specification of the frequency denominators in Eq. (2). Substitution of $|\mathcal{D}(\omega)| = \hbar\Gamma_{\text{MD}} \sim 0.05$ eV (from the experiments), and $|\mathcal{D}(2\omega)| = \hbar\Gamma_{\text{ED}} \sim 0.23$ eV (from Ref. [17]) yields an unscreened bulk susceptibility of $\chi_4^{(Q)} \sim 1.2 \times 10^{-12}$ esu. This is in reasonable agreement with the experimentally obtained $\chi_4^{(Q)} = 1.4 \times 10^{-13}$ esu, taking into account estimations of the so far neglected screening and local field effects [13].

Normally a strong quadrupole bulk contribution also leads to a strong effective interface dipole susceptibility via the strong field gradients at the interface [10,12]. However, since only the $\chi_1^{(Q)}$ and $\chi_2^{(Q)}$ tensor component are involved in the field gradient induced surface susceptibility, which are just forbidden components for the MD contribution, the dominance of the MD processes is a natural way to explain the minor role of any surface and interface tensor component. Furthermore, contributions proportional to $\nabla \cdot \vec{\chi}^{(Q)}$ at the interface [10] are only of importance if the electric dipole forbidden transition occurs at 2ω , which is not the case for our resonant C_{60} study.

In conclusion, we fully described the origin of the SHG resonance for C_{60} at $2\hbar\omega = 3.60$ eV. We demonstrated the dominant role of the MD induced contribution, which was confirmed by the LCAO calculation. The strength of the SH response of C_{60} is illustrated by the notion that $[n(\omega)\omega/c]\chi_3^{(Q)} = 1.8 \times 10^{-8}$ esu for C_{60} is an order of magnitude larger than the electric dipole allowed (but nonresonant) $\chi_{xxx}^{(2)} = 1.9 \times 10^{-9}$ esu of noncentrosymmetric quartz. The reason that particularly C_{60} shows such a strong MD induced SHG is related to the spherical shape of the molecules, with a large radius, and the presence of a diagram with two levels of the same l quantum number, split such that a double resonance is possible.

We outlined a systematic method for the full separation of all tensor components in the thin film geometry. As shown for the C_{60} experiment, the method can also be reversed. Once having a strong indication that bulk processes are dominant, the thin film experiment yields information about the MD or EQ character of the bulk SHG. Both applications of the presented general method might show their value to many other thin film systems.

We would like to acknowledge useful discussions with

Professor Y. R. Shen and Dr. D. Johannsmann. This investigation was supported by the Netherlands Foundation for Fundamental Research on Matter (FOM) with financial support from the Netherlands Organization for the Advancement of Pure Research (NWO).

-
- [1] J. S. Meth, H. Vanherzeele, and Y. Wang, Chem. Phys. Lett. **197**, 26 (1992).
 - [2] Z. H. Kafafi, J. R. Lindle, R. G. S. Pong, F. J. Bartoli, L. J. Lingg, and J. Milliken, Chem. Phys. Lett. **188**, 492 (1992).
 - [3] Y. Wang and L. T. Cheng, J. Phys. Chem. **96**, 1530 (1992).
 - [4] H. Hoshi, N. Nakamura, Y. Maruyama, T. Nakagawa, S. Suzuki, H. Shiromaru, and Y. Achiba, Jpn. J. Appl. Phys. **30**, L1397 (1991).
 - [5] X. K. Wang, T. G. Zhang, W. P. Li, S. Z. Liu, G. K. Wong, M. M. Kappes, R. P. H. Chang, and J. B. Ketterson, Appl. Phys. Lett. **60**, 810 (1992).
 - [6] B. Koopmans, A. Anema, H. T. Jonkman, G. A. Sawatzky, and F. van der Woude, Phys. Rev. B **48**, 2759 (1993).
 - [7] J. E. Sipe, V. Mizrahi, and G. I. Stegeman, Phys. Rev. B **35**, 9091 (1987).
 - [8] S. Leach, M. Vervloet, A. Desprès, E. Bréheret, J. P. Hare, T. J. Dennis, H. W. Kroto, R. G. Taylor, and D. R. M. Walton, Chem. Phys. **160**, 451 (1992).
 - [9] G. F. Bertsch, A. Bulgac, D. Tománek, and Y. Wang, Phys. Rev. Lett. **67**, 2690 (1991).
 - [10] P. Guyost-Sionnest and Y. R. Shen, Phys. Rev. B **38**, 7985 (1988).
 - [11] V. Mizrahi and J. E. Sipe, J. Opt. Soc. Am. B **5**, 660 (1988).
 - [12] P. Guyot-Sionnest, W. Chen, and Y. R. Shen, Phys. Rev. B **33**, 8254 (1986).
 - [13] B. Koopmans, G. A. Sawatzky, and F. van der Woude (to be published); B. Koopmans, thesis, University of Groningen, The Netherlands, 1993.
 - [14] N. Bloembergen, R. K. Chang, S. S. Jha, and C. H. Lee, Phys. Rev. **174**, 813 (1968).
 - [15] In Ref. [6] we find the resonant SHG to be 90° out of phase with a nonresonant surface contribution of the substrate. Because of the 90° phase difference between bulk contributions of a very thin film (6 nm in the experiments) and corresponding surface contributions, this indicates a real bulk susceptibility exactly at resonance, and as a consequence, a doubly resonant process.
 - [16] The "esu" unit for $\vec{\chi}_s^{(D)}$, $\vec{\chi}_l^{(D)}$, and $\vec{\chi}^{(Q)}$ is $\text{cm}^2/\text{statvolt}$.
 - [17] S. L. Ren, Y. Wang, A. M. Rao, E. McRae, J. M. Holden, T. Hager, K. Wang, W. T. Lee, H. F. Ni, J. Selegue, and P. C. Ecklund, Appl. Phys. Lett. **59**, 2678 (1991).